ENVIRONMENTAL RESEARCH
LETTERS

PURPOSE-LED PUBLISHING™
Celebrating the 20th anniversary of Environmental Research Letters

LETTER • **OPEN ACCESS**

Present and future land surface and wet bulb temperatures in the Arabian Peninsula

To cite this article: S Safieddine *et al* 2022 *Environ. Res. Lett.* **17** 044029

View the article online for updates and enhancements.

You may also like

- Escalating global exposure to compound heat-humidity extremes with warming
Dawei Li, Jiacan Yuan and Robert E Kopp
- Changes in regional wet heatwave in Eurasia during summer (1979–2017)
Shuang Yu, Simon F B Tett, Nicolas Freychet et al.
- Estimating heat stress from climate-based indicators: present-day biases and future spreads in the CMIP5 global climate model ensemble
Y Zhao, A Ducharne, B Sultan et al.

This content was downloaded from IP address 158.69.193.207 on 07/11/2026 at 02:49

IOP Publishing Environ. Res. Lett. 17 (2022) 044029 https://doi.org/10.1088/1748-9326/ac507c

ENVIRONMENTAL RESEARCH
LETTERS

LETTER

Present and future land surface and wet bulb temperatures in the Arabian Peninsula

S Safieddine[1,*], C Clerbaux[1,2], L Clarisse[2], S Whitburn[2] and E A B Eltahir[3]

[1] LATMOS/IPSL, Sorbonne Université, UVSQ, CNRS, Paris, France
[2] Université libre de Bruxelles (ULB), Spectroscopy, Quantum Chemistry and Atmospheric Remote Sensing (SQUARES), Brussels, Belgium
[3] Ralph M. Parsons Laboratory, Massachusetts Institute of Technology, Cambridge, MA 02139, United States of America
* Author to whom any correspondence should be addressed.

E-mail: sarah.safieddine@latmos.ipsl.fr

Keywords: Arabian Peninsula, land surface temperature, wet bulb temperature, extreme heat, IASI, ERA5, climate projections

OPEN ACCESS

RECEIVED
24 November 2021

REVISED
19 January 2022

ACCEPTED FOR PUBLICATION
31 January 2022

PUBLISHED
18 March 2022

Original content from this work may be used under the terms of the Creative Commons Attribution 4.0 licence.

Any further distribution of this work must maintain attribution to the author(s) and the title of the work, journal citation and DOI.

Abstract

The Arabian Peninsula exhibits extreme hot summers and has one of the world's largest population growths. We use satellite observations and reanalysis as well as climate model projections to analyze morning and evening land surface temperatures (LSTs), to refer to processes at the surface, and wet bulb temperatures (WBTs) to measure human heat stress. We focus on three regions: the Persian Gulf and Gulf of Oman, the inland capital of Saudi Arabia, Riyadh and the irrigated agricultural region in Al-Jouf, Saudi Arabia. This study shows that the time of day is important when studying LST and WBT, with current and future WBT higher in the early summer evenings. It also shows that the effect of humidity brought from waterbodies or through irrigation can significantly increase heat stress. Over the coasts of the Peninsula, humidity decreases LST but increases heat stress via WBT values higher than 25 °C in the evening. Riyadh, located in the heart of the Peninsula has lower WBT of 15 °C–17.5 °C and LST reaching 42.5 °C. Irrigation in the Al-Jouf province decreases LST by up to 10° with respect to its surroundings, while it increases WBT by up to 2.5°. Climate projections over the Arabian Peninsula suggest that global efforts will determine the survivability in this region. The projected increase in LST and WBT are +6 °C and +4 °C, respectively, in the Persian Gulf and Riyadh by the end of the century, posing significant risks on human survivability in the Peninsula unless strict climate mitigation takes place.

1. Introduction

Most land regions are experiencing greater warming than the global average temperature increase [1], and the projections of future temperatures have large regional and local uncertainties since models fail in the representation of local land processes [2]. This poses some important limitations on the accuracy of these projections on a local scale and as such, their societal/epidemiological impacts such as those of temperature extremes [3]. From here stems the need to understand the important variables for the feedback between land and atmosphere, and their effect on human survivability under extreme heat conditions. We present here two variables that can help us understand this complex relationship in a region with extreme heat in summer, the Arabian Peninsula: the land surface temperature (LST) and the wet bulb temperature (WBT).

LST relates to the thermal radiation emitted by the Earth's surface, from depths as small as 10–20 micrometers [4]. It is usually obtained from remote sensing data. Differences between LST and atmospheric near surface temperature can be large under cloud-free, low wind speed conditions since land heats much faster than air, and smaller under cloudy conditions or when solar insolation is low [5]. It is an important factor for studying the Earth's energy balance, convection at the surface, monitoring droughts, land use, and surface urban heat islands (SUHI) [6, 7]. SUHIs exist when the temperature of the surface is warmer in urban areas than in rural surroundings [8]. The inverse phenomenon is the surface urban cool island (SUCI) effect and is common to dry and arid climates: the city is cooler than its surrounding. This has been detected in many cities in dry climates around the world [9], and in many metropolitans of the Arabian Peninsula, such as the cities of Kuwait

© 2022 The Author(s). Published by IOP Publishing Ltd

[10], Riyadh [11], or Dubai [9]. Sand's temperature can be extremely high during sunny summer days: it has very low water content and a fast depletion rate of water via evaporation. Sand holds less water than other materials and has smaller thermal inertia. Over the surface, low relative humidity enhances the dryness and heat exacerbating soil aridity in the upper layers of the sand. LST has been identified as one of the most significant factors that can influence SUHI/SUCI phenomena [12, 13]. Studies have shown that urban development incorporating vegetation could be a primary strategy to mitigate SUHI [14]. However, vegetation, especially in arid regions, requires irrigation, which adds humidity to the atmosphere. Humidity is also brought naturally from the sea to coastal regions, and the Arabian Peninsula is surrounded by bodies of water: The Red Sea to the west and southwest, the Persian Gulf and the Gulf of Oman to the northeast, and the Arabian Sea and the Indian Ocean to the southeast. A good metric to assess the combined effect of humidity and temperature to the coasts of the peninsula is the WBT. It depends both on air temperature (also called dry bulb temperature) and air humidity near the surface. It is important in the context of extreme heat, as it reflects the body's limited ability to efficiently shed heat. Heat episodes with high WBT can be dangerous to a human's health and lower the productivity of outdoor laborers [15, 16]. Any exceedance of 35 °C for extended periods will induce hyperthermia as dissipation of body metabolic heat becomes impossible. It is therefore a measure of heat stress and current available observations show that it rarely exceeds 31 °C [17].

The Arabian Peninsula is a region of extreme heat in summer, and is a center of demographic, and urban development as it is the world's single largest source of petroleum. Economic expansion in countries like Saudi Arabia, United Arab Emirates, Kuwait, Oman, Qatar and Bahrain has encouraged millions of migrants to move to the Middle East for work. Under climate change stress, and the influx of population to this region, this study aims to understand the effects of geographical location and land use on current and future summer (June–August) heat stress, during day and night separately, and their implications, which should be taken into account in urban development strategies.

2. Methods

2.1. Infared atmospheric sounding interferometer (IASI) LST

The LST product used in this work is provided by the family of the IASI instruments [18], on board of the Eumetsat (European Organisation for the Exploitation of Meteorological Satellites) Metop series of polar orbiting satellites: Metop-A, launched in 2006, Metop-B launched in 2012, and Metop-C launched in 2018. Each instrument has a morning and an evening orbit at around 9:30 AM and PM. IASI measures calibrated radiances in the thermal infrared spectral range, at a global scale and revisiting all points on the Earth's surface twice a day. In spectral bands where no gas absorbs, accurate information on the surface properties and temperature is derived. The latter is a clear-sky product retrieved using a method based on entropy reduction/information theory and neural networks [19]. Validation of this product with other datasets (satellite and ground-based measurements) shows that it is suitable for trend analysis and to check for local and regional variations of temperature in different regions of the world [19]. In order to achieve a higher resolution for spatial coverage, we averaged the IASI LST using an oversampling method, widely used in other studies for various trace gas concentrations using different instruments [20–22] but until now, never for temperature analysis with IASI. The three instruments are cross validated for temperature and show excellent agreement [23]. Metop-A was decommissioned in 2017. In this work, a combination of the three instruments' products are used for the summers of 2008–2020.

2.2. WBT

The WBT is a nonlinear function of temperature and humidity near the surface. In this work we use the formula of WBT provided by Davies-Jones [24]. Near surface temperature and humidity used to calculate WBT are provided by the European Center for Medium Weather Forecast (ECMWF)'s latest reanalysis ERA5 [25]. ERA5 datasets are at $0.25° \times 0.25°$ resolution (native horizontal resolution of ERA5 is ∼31 km). All different retrieved variables are interpolated in time and space to match the IASI morning and evening observations. We do not use the LST from ERA5, since the super sampling method of IASI data leads to much finer resolution (of around $0.01° \times 0.01°$) as the figures 1–3 show. ERA5 assimilates IASI radiances, and the two datasets agree very well as shown by Safieddine *et al* [19] and Bouillon *et al* [23].

2.3. EC-Earth climate model

The reanalysis uses the ECMWF's Integrated Forecasting System for the atmosphere–land component (IFS). IFS is also used by the European Earth Consortium climate model (EC-Earth, www.ec-earth.org/). It is complemented with other model components to simulate the full range of Earth system interactions that are relevant to climate [26]. The model participates in CMIP6 [27] (Climate model intercomparison project, phase 6, part of the Intergovernmental Panel on Climate Change (IPCC) report of 2021 [1]) with different model configurations. Here we use the Scenario Model Intercomparison Project (ScenarioMIP), covering the period 2015–2100. We note that the versions of the IFS models used in ERA5 and in EC-Earth

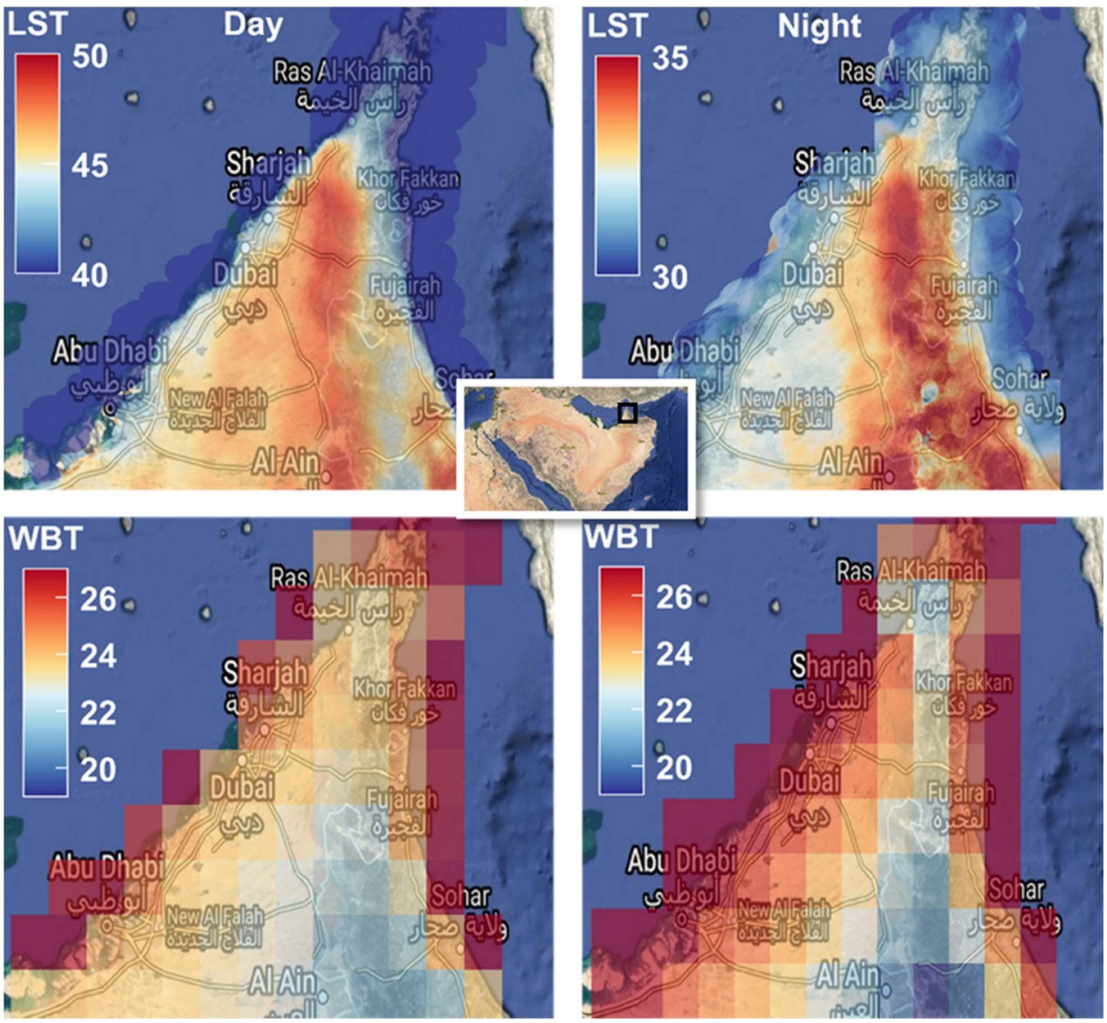


Figure 1. Upper panel: IASI day and night observations of LST during summer (June–August) for the cities on the Persian Gulf and the Gulf of Oman. Lower panel: ERA5 WBT interpolated to the time and location of IASI's observation. Note that the color bar limits for LST differ in each of the panels.

are not identical. EC-Earth branched off to include its own additions for climate purposes. Moreover, EC-Earth is not assimilated and is not initialized with observations several times a day like ERA5. Therefore, we do not attempt to validate EC-Earth with ERA5. In this work, we use the simulations from two shared socio-economic pathways (SSPs) [28]: the SSP2-4.5 corresponds to 'middle of the road/sustainability' socio-economic family with a nominal 4.5 W m^{-2} radiative forcing level by 2100, and the SSP5-8.5 (8.5 W m^{-2}) marks the upper edge of the SSP scenario spectrum with a high reference scenario in a high fossil-fuel developed world throughout the 21st century.

3. Results

3.1. Local diurnal variation of LST and WBT

The Arabian Peninsula is well targeted since the cloud cover over this region during summer is negligible, giving IASI frequent access to the surface in order to derive clear-sky LST. We focus on the summer season since it is the most relevant for human heat stress. We calculate WBT from the ERA5 temperature and humidity interpolated in time and space to the IASI morning and evening available observations (9:30 AM and PM). We focus on three distinct regions: the 1st is coastal, the Persian Gulf and the Gulf of Oman. The second is Riyadh, the capital of Saudi Arabia, ∼500 km away from the coast, and the third is a large agricultural region in Saudi Arabia, in Al-Jouf province. The location of the three region is shown in figure 4, panel (i).

3.1.1. The Persian Gulf and the Gulf of Oman

Figure 1 shows the morning (labeled 'Day') and evening ('Night') LST and WBT over the Persian Gulf and the Gulf of Oman. We chose this region because it has major coastal cities (such as Sharjah, Dubai, and Abu Dhabi) with high population densities, and the city of Al-Ain which is a major in-land city of the Abu Dhabi province. The LST is 40 °C–45 °C close to the

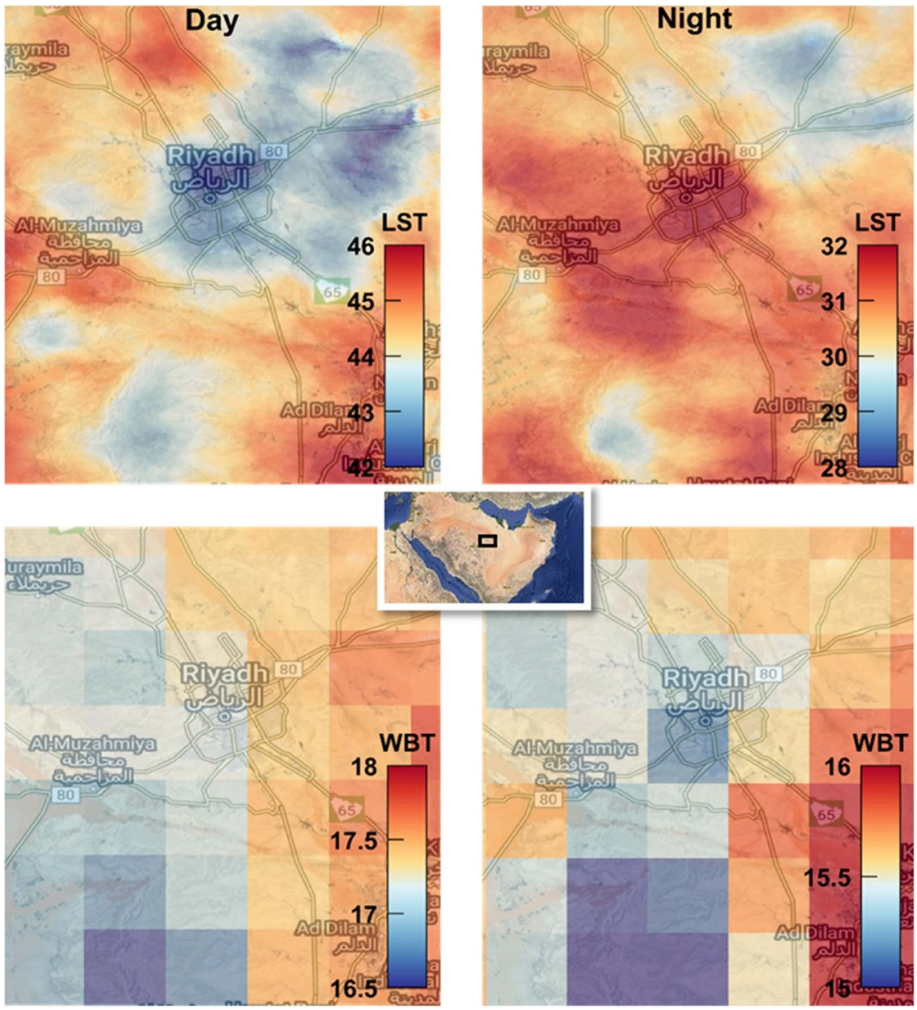


Figure 2. Same as figure 1 but for Riyadh. The capital is located in the desert of the Arabian Peninsula and acts as an urban cool island during the day and as an urban heat island during the night. WBT values are lower than those over the Persian Gulf. Note that the limits of the temperature scales vary in each of the panels.

coasts, lower than the inland values as the sea breeze transfers cooler air to the adjacent areas of the coast and enhances wind speed. LST is higher during the day, and smaller during the summer nights, since it is largely dependent on solar radiation. LST increases as the distance from the coast increases, approaching 50 °C during the day and 35 °C during the night. We note that other factors can play a significant role in increasing or decreasing LST, including elevation, and the presence of green areas [11].

The WBT for the coastal cities (23 °C–26 °C) is much higher than the inland WBT both during the day and the night. The city of Al-Ain for example, has high LST but a WBT lower by 3°–6° than those recorded at the coastal cities. This clearly shows the dependence of the WBT on the relative humidity (and time of the day). In the evening, the heat stress (WBT) is higher since it corresponds to around 9:30 PM, with land–sea exchanges saturating the air with humidity, affecting human's heat comfort during population leisure time.

3.1.2. Riyadh

In figure 2, we show the day and night LST and WBT over Riyadh as an example of non-coastal city. Riyadh, during the day, acts as a SUCI, as the upper left panel of figure 2 shows. With high solar radiation in summer, the desert sand becomes very hot. However, the city's landscape is cooler. This has been seen in previous studies for Riyadh, using different other instruments [11, 29]. At night, the desert/arid regions cool faster than the urban city, and Riyadh becomes a typical SUHI. In most climates, including arid regions, SUHI are prominent at night because street canyons tend to trap heat in addition to urban materials that have slower nighttime cooling rate than natural surfaces [9]. The lower panel shows the WBT calculated from ERA5. *In situ* measurements of WBTs recorded a summer average of 18.8 °C [30]. We can see that the derived WBT here is slightly lower, probably due to the grid size (31 km), and is of 17 °C–17.5 °C in the morning of summer days, and between 15 °C and 16 °C during summer

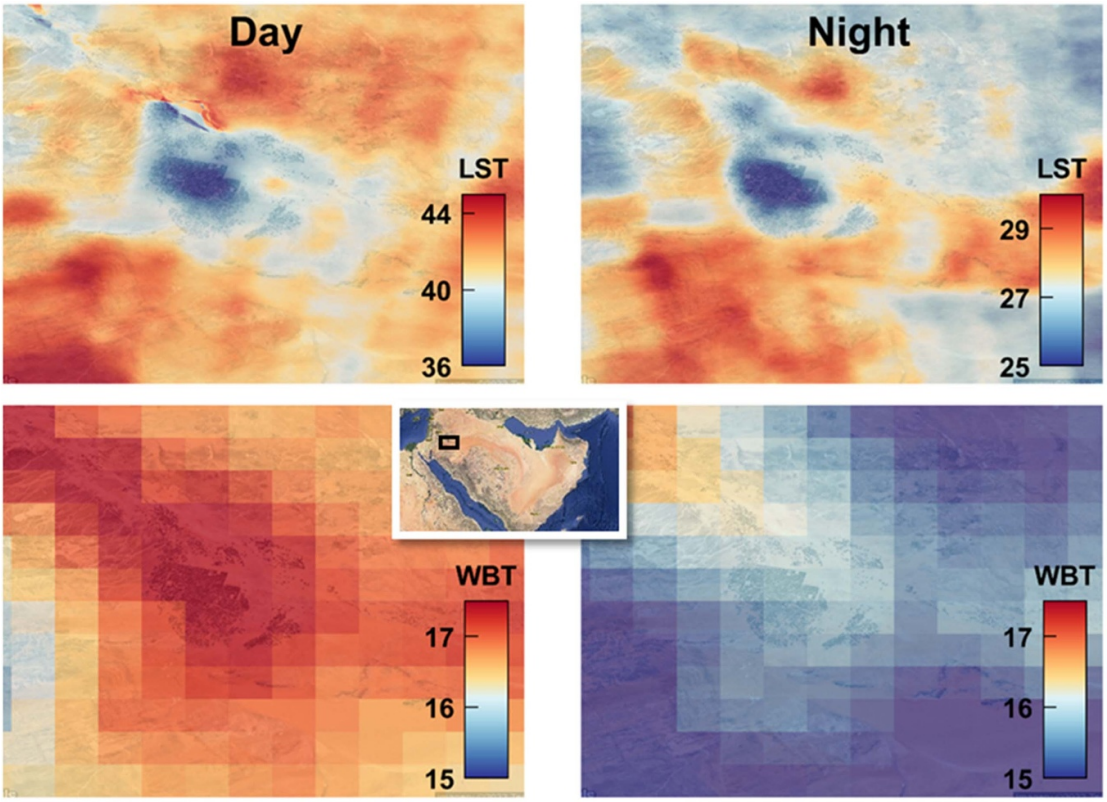


Figure 3. Same as figures 1 and 2 but for the Al-Jouf agricultural region. Irrigation decreases LST but increases the heat stress through the increase in humidity near the surface.

nights. The resolution of ERA's WBT, while the best available reanalysis resolution available today, does not show a hotspot/coolspot concentrated over Riyadh itself. Nevertheless, the low humidity, which is common for in-land regions such as Riyadh, makes the heat stress, reflected in the WBT, lower on average. This is even recorded at night, when Riyadh acts as a SUHI.

3.1.3. Al-Jouf agricultural region

Al-Jouf is characterized by hot desert climatic conditions and is one of the largest agricultural regions in Saudi Arabia. Agriculture in this region is heavily irrigated and primarily depends on limited non-renewable groundwater sources [31]. This irrigation therefore affects the surface and near-surface properties that are reflected in figure 3 with the LST and WBT. Since the fields are irrigated, LST is lower. The soil has higher water content which cools the surface. Vegetation also increases latent heat flux to the atmosphere through increased evaporative surface area and transpiration [14]. This is particularly clear over the center of this cultivated parcel of land shown in figure 3. Over the whole domain, LST is lower at night, due to the lack of solar radiation heating the surface. Analysis of LST during each of the summer months (not shown here), suggests that irrigation is broadly constant all summer long over all of the crops shown here, as the region accounts for a numerous distinct variety of crops [32]. On the other hand, the lower panel with the WBT shows an opposite effect: the heat stress is higher with higher WBT above and near the agricultural fields. This is mainly driven by the higher relative humidity from irrigation over the fields. Higher humidity and smaller temperatures over the fields makes the WBT humidity-limited. This is particularly seen during the day, as irrigation is recommended in the early morning, when temperature and wind speed are the lowest [33]. Humidity in this case plays a big role in determining the heat comfort near irrigated land. On average, the figure shows that irrigation can increase the heat stress by 2° and 3° with respect to its surrounding.

4. Mid- to end-century projections of regional LST and WBT

We focus now on the mid to end of century evolution of the summertime LST and WBT over this region under a 'sustainable future' scenario (SSP 2–4.5) and a 'fossil fuel development' SSP 5–8.5 scenario (section 2.3). With this, we can check the climate response of the present day observations/reanalysis of LST and WBT from IASI and ERA5 to different mitigation strategies. In fact, we do not attempt to validate the 'present day' EC-Earth with that from IASI or ERA5 since over each of the three regions studied in section 3, the local fine land processes

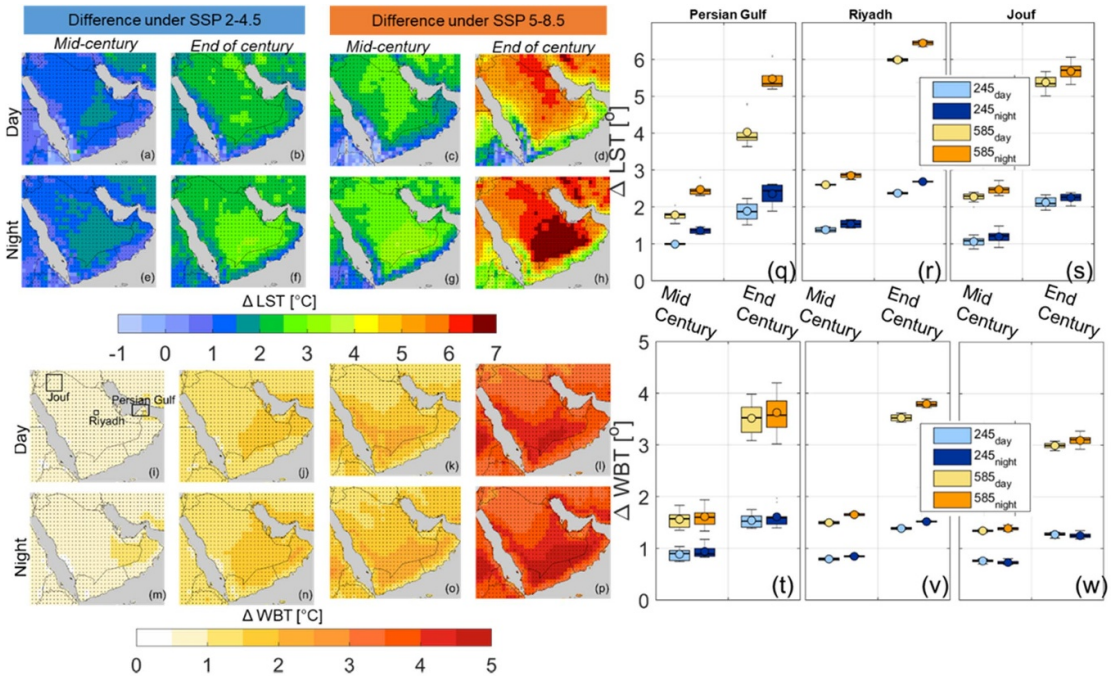


Figure 4. Panels (a)–(p): mean change in day and night LST (upper panels) and WBT (lower panels) in mid-century (2045–2069) and end of century (2075–2099) with respect to the present day (2015–2039), under two different SSPs from the EC-Earth model. The dotted areas indicate statistical significance with 95% confidence from a Student's *t* test. Panels (q)–(w): box plot of the mean change in LST and WBT in the three regions discussed in the study (locations are shown on panel (i)). The central black line indicates the median, the circle is the mean, and the bottom and top edges of the box indicate the 25th and 75th percentiles. The whiskers extend to the most extreme data.

might not be represented in the model. The urban heat/cool island effect or coast/land interaction in Riyadh and the Persian Gulf are much smaller than the model resolution (which is around 0.7° × 0.7°), and irrigation in Al-Jouf is not included in EC-Earth (as for many other climate models). Irrigation forecast remains very challenging as it depends on the evolution of soil, vegetation, water availability, expansion and shifts of agricultural practices. This clearly limits its ability to predict future WBT in Al-Jouf and more generally everywhere else in the Peninsula. Moreover, the spatial resolution of the ERA5 or the EC-Earth dataset might not capture all meso- and micro-scale variations of meteorological conditions, such as mesoscale convective systems [34], especially in areas with a complex orography, land cover, or near the coasts [35, 36]. Even at the smallest grid cell, the simulation output is a collection of values averaged over an area. As such, it depends on grid cell size, the terrain complexity and the type of surface.

For all these reasons, the simulation used here, will tell us the climate response on the longer term without taking into account local land use changes. Since we calculate the difference between different climate periods, the increase can therefore be projected onto present-day values from IASI and ERA5.

We show in figure 4 the mean change during the day (morning 3 h average, corresponding to 9 to 12 PM local time) and during the night (3 h average, from 9 PM to midnight local time) of LST and WBT in the 25 year average climate representing mid-century (2045–2069) and that at the end of the century (2075–2099) with respect to present day climate (2015–2039) under two different SSPs. The end of century increase in SSP2-4.5 is relatively close to that reached by mid-century for SSP5-8.5. The latter shows a grim increase in 2100 reaching +7° for LST (panels (d) and (h)) and +5° (panels (l) and (p)) for WBT respectively, in southern Saudi Arabia and northern Oman and Yemen. What can be noted is that the future increase in LST and WBT can be higher at night than during the day. By the early evening, land would have stored all the heat from sunlight (high LST) and the atmosphere in coastal areas would have been also saturated with moisture (high temperature and humidity).

Panels (q)–(w) show the same mean change for the regions discussed in section 3 (rectangles in panel (i)): the Persian Gulf, Riyadh, and Al-Jouf. The average increase in summertime LST and WBT is more or less of the same magnitude for the three regions in particular for the SSP2-4.5 scenario. This is due to the fact that the we are checking the regional climate response. Moreover, relative humidity remains mostly constant over this region under the different SSPs; a result that is expected on climatological time scales [1, 37, 38], particularly over mid-latitude

regions of the Northern Hemisphere. Therefore, the increase in WBT is temperature-limited and as such is similar in regions close in latitudes.

Panels (q)–(w) show that for the SSP2-4.5 scenario, and by mid-century, the increase in LST for the three regions is between +1 and 1.6, and lower than +1 °C for WBT for all three regions (median values). By the end of the century, and for the same scenario, the increase in LST is between +2 °C and +3 °C and is close to +1.5 °C for WBT. The increase in LST is much more enhanced for the SSP5-8.5 scenario. By mid-century, it is between +1.8 °C (day, Persian Gulf) and +3 °C (day, Riyadh). For WBT, it is between +1 °C and +2 °C for the three regions investigated (median values). In 2100, LST reaches an increase close to or larger than +6° (Riyadh, at night), and WBT increases by more than +3° for all the regions investigated. LST and WBT are both higher in the evening than in the morning. This increase in WBT in the Persian Gulf and the Gulf of Oman would make average WBT, as compared to figure 1, close to or higher than 30 °C. An increase of this magnitude in WBT would possibly lead to premature death of the weakest, namely children and elderly [17].

5. Discussion and conclusions

We investigate in this study the current and future LST and WBT over the Arabian Peninsula. Using high resolution LST observations from IASI satellite measurements and WBT calculated from reanalysis data from ERA5, the hottest temperatures recorded during the summer days are those over the desert/arid regions due to lack of soil water content, sparse vegetation cover, and very low relative humidity above the surface. For WBT, areas close to the coasts have higher values because they are more humid. Increasing urbanization, evolving urban landscapes, and growing populations are changing the land cover and the land-atmosphere energy fluxes exchanges. This paper highlights two main points to be considered in designing future land use over this region:

(a) LST and WBT change with the time of the day. The diurnal difference effect is highlighted in Riyadh being a SUCI during the day, and a SUHI at night. For WBT, the cities on the Persian Gulf have higher current and future WBT in early evenings of the summer (air saturated with humidity), when people tend to go out. It is important to consider these diurnal effects, to properly assess future climatic effects on LST and WBT and their effect on outdoor activities at different times of the day.
(b) Irrigation increases heat stress. Vegetated spaces can reduce the surface and near surface temperatures through evapotranspiration and shade and is highlighted in many studies as a strategy to reduce the intensities of SUHIs [39, 40]. However, vegetation in arid regions requires irrigation and we show here that irrigation enhances the heat stress with an increase in WBT reaching +2 °C with respect to the surroundings (figure 3). The planned Saudi Green Initiative aims at planting 50 billion trees in Saudi Arabia (www.saudigreeninitiative.org/). The choice of vegetation in populated region is therefore important. For example, it is better to choose native or drought tolerant species that requires less irrigation. Moreover, irrigation should be included in future climate projections as it plays an essential role in determining future heat stress and survivability in populated regions of the world.

The alarming future increase in temperatures in the Arabian Peninsula and shown in this work would constrain major socio-economic development in cities on the Persian Gulf, Gulf of Oman and the Red Sea. Even for the sustainable scenario, the high WBT poses significant risk on outdoor activities and labor (such as constructing workers) even at night. This region would considerably benefit from strict mitigation effort to reduce the severity of the projected impact of climate change.

Data availability statement

All data that support the findings of this study are included within the article (and any supplementary files).

IASI land surface temperature (also called Earth's 'skin temperature') data are available on https://iasi-ft.eu/. ERA5 data (t2m, d2m, skin temperature/LST and surface pressure) used in this work to calculate WBT are available from the Climate Data Store at the following DOI: https://doi.org/10.24381/cds.adbb2d47.

EC-Earth3 model output prepared for CMIP6 ScenarioMIP are retrieved here: https://doi.org/10.22033/ESGF/CMIP6.727.

Acknowledgments

This project has received funding from the European Research Council (ERC) under the European Union's Horizon 2020 and innovation programme (Grant Agreement No. 742909). The IASI mission is a joint mission of Eumetsat and the Centre National d'Etudes Spatiales (CNES, France). The IASI L1 data are distributed in near real time by Eumetsat through the Eumetcast system distribution. The authors acknowledge the Aeris data infrastructure for providing the IASI L1C data. The authors thank M D Boucher and D Coppens for the reprocessed L1C IASI radiances used to compute LST, and thank V Pellet, F Aires, G Levavasseur, Y-W Choi, and R Döscher for useful discussions.

ORCID iD

S Safieddine https://orcid.org/0000-0002-8947-7950

References

[1] Masson-Delmotte V *et al* 2021 *IPCC, 2021: Climate Change 2021: the Physical Science Basis Contribution of Working Group I to the Sixth Assessment Report of the Intergovernmental Panel on Climate Change* Chapter 2 (Cambridge: Cambridge University Press) accepted

[2] Vogel M M *et al* 2017 Regional amplification of projected changes in extreme temperatures strongly controlled by soil moisture-temperature feedbacks *Geophys. Res. Lett.* **44** 1511–9

[3] Pal J S and Eltahir E A B 2016 Future temperature in southwest Asia projected to exceed a threshold for human adaptability *Nat. Clim. Change* **6** 197–200

[4] McKeown W, Bretherton F, Huang H L, Smith W L and Revercomb H L 1995 Sounding the skin of water: sensing air–water interface temperature gradients with interferometry *J. Atmos. Oceanic Technol.* **12** 1313–27

[5] Good E J 2016 An *in situ*-based analysis of the relationship between land surface "skin" and screen-level air temperatures *J. Geophys. Res.* **121** 8801–19

[6] Rhee J, Im J and Carbone G J 2010 Monitoring agricultural drought for arid and humid regions using multi-sensor remote sensing data *Remote Sens. Environ.* **114** 2875–87

[7] Zhou L *et al* 2003 A sensitivity study of climate and energy balance simulations with use of satellite-derived emissivity data over Northern Africa and the Arabian Peninsula *J. Geophys. Res.* **108** D24

[8] Voogt J A and Oke T R 2003 Thermal remote sensing of urban climates *Remote Sens. Environ.* **86** 370–84

[9] Dialesandro J M, Wheeler S M and Abunnasr Y 2019 Urban heat island behaviors in dryland regions *Environ. Res. Commun.* **1** 081005

[10] Alahmad B, Tomasso L P, Al-Hemoud A, James P and Koutrakis P 2020 Spatial distribution of land surface temperatures in Kuwait: urban heat and cool islands *Int. J. Environ. Res. Public Health* **17** 9

[11] Abulibdeh A 2021 Analysis of urban heat island characteristics and mitigation strategies for eight arid and semi-arid gulf region cities *Environ. Earth Sci.* **80** 259

[12] Song J, Du S, Feng X and Guo L 2014 The relationships between landscape compositions and land surface temperature: quantifying their resolution sensitivity with spatial regression models *Landscape Urban Plan.* **123** 145–57

[13] Zhou W, Huang G and Cadenasso M L 2011 Does spatial configuration matter? Understanding the effects of land cover pattern on land surface temperature in urban landscapes *Landscape Urban Plan.* **102** 54–63

[14] Akbari H 1992 Cooling our communities *A Guidebook on Tree Planting and Light-Colored Surfacing* 24 February (Washington, DC: U.S. Environmental Protection Agency, Office of Policy Analysis, Climate Change Division) p 27 (available at: https://escholarship.org/uc/item/98z8p10x) (Accessed 10 March 2022)

[15] Mora C *et al* 2017 Global risk of deadly heat *Nat. Clim. Change* **7** 501–6

[16] Raymond C, Matthews T and Horton R M 2020 The emergence of heat and humidity too severe for human tolerance *Sci. Adv.* **6** 19

[17] Sherwood S C and Huber M 2010 An adaptability limit to climate change due to heat stress *Proc. Natl Acad. Sci.* **107** 9552–5

[18] Clerbaux C *et al* 2009 Monitoring of atmospheric composition using the thermal infrared IASI/MetOp sounder *Atmos. Chem. Phys.* **9** 6041–54

[19] Safieddine S *et al* 2020 Artificial neural networks to retrieve land and sea skin temperature from IASI *Remote Sens.* **12** 2777

[20] Clarisse L *et al* 2019 Atmospheric ammonia (NH_3) emanations from Lake Natron's saline mudflats *Sci. Rep.* **9** 4441

[21] de Foy B, Lu Z, Streets D G, Lamsal L N and Duncan B N 2015 Estimates of power plant NO_x emissions and lifetimes from OMI NO_2 satellite retrievals *Atmos. Environ.* **116** 1–11

[22] Fioletov V E, McLinden C A, Krotkov N, Moran M D and Yang K 2011 Estimation of SO_2 emissions using OMI retrievals *Geophys. Res. Lett.* **38** 21

[23] Bouillon M *et al* 2020 Ten-year assessment of iasi radiance and temperature *Remote Sens.* **12** 2393

[24] Davies-Jones R 2008 An efficient and accurate method for computing the wet-bulb temperature along pseudoadiabats *Mon. Weather Rev.* **136** 2764–85

[25] Hersbach H *et al* 2020 The ERA5 global reanalysis *Q. J. R. Meteorol. Soc.* **146** 1999–2049

[26] Döscher R *et al* The EC-Earth3 Earth system model for the climate model intercomparison project 6 *Geosci. Model Dev. Discuss.* 1–90 (in review)

[27] Eyring V *et al* 2016 Overview of the coupled model intercomparison project phase 6 (CMIP6) experimental design and organization *Geosci. Model Dev.* **9** 1937–58

[28] Riahi K *et al* 2017 The shared socioeconomic pathways and their energy, land use, and greenhouse gas emissions implications: an overview *Glob. Environ. Change* **42** 153–68

[29] Aina Y A, Adam E M and Ahmed F 2017 Spationtemporal variations in the impacts of urban land use types on urban heat island effects: the case of Riyadh, Saudi Arabia *The Int. Archives of the Photogrammetry, Remote Sensing and Spatial Information Sciences* vol XLII-3-W2 (Copernicus GmbH) pp 9–14

[30] Alshenaifi M A and Sharples S 2019 A parametric analysis of the influence of wind speed and direction on the thermal comfort performance of a passive downdraught evaporative cooling (PDEC) system—field measurements from a Saudi Arabian library *IOP Conf. Ser.: Earth Environ. Sci.* **329** 012042

[31] Youssef A M, Abu Abdullah M M, Pradhan B and Gaber A F D 2019 Agriculture sprawl assessment using multi-temporal remote sensing images and its environmental impact; Al-Jouf, KSA *Sustainability* **11** 4177

[32] Sdurayhem 2019 Agricultural production survey methodology *General Authority for Statistics* 29 September (available at: www.stats.gov.sa/en/1060-0) (Accessed 3 January 2022)

[33] Al-Ghobari H and Dewidar A Z 2021 A comparative study of standard center pivot and growers-based modified center pivot for evaluating uniformity coefficient and water distribution *Agronomy* **11** 1675

[34] Belmonte Rivas M and Stoffelen A 2019 Characterizing ERA-Interim and ERA5 surface wind biases using ASCAT *Ocean Sci.* **15** 831–52

[35] Luo H *et al* 2019 Assessment of ECMWF reanalysis data in complex terrain: can the CERA-20C and ERA-Interim data sets replicate the variation in surface air temperatures over Sichuan, China? *Int. J. Climatol.* **39** 5619–34

[36] Thomas S R, Nicolau S, Martínez-Alvarado O, Drew D J and Bloomfield H C 2021 How well do atmospheric reanalyses reproduce observed winds in coastal regions of Mexico? *Meteorol. Appl.* **28** e2023

[37] Simmons A J, Willett K M, Jones P D, Thorne P W and Dee D P 2010 Low-frequency variations in surface

atmospheric humidity, temperature, and precipitation: inferences from reanalyses and monthly gridded observational data sets *J. Geophys. Res.* **115** D1

[38] Dunn R J H, Willett K M, Ciavarella A and Stott P A 2017 Comparison of land surface humidity between observations and CMIP5 models *Earth Syst. Dyn.* **8** 719–47

[39] Bowler D E, Buyung-Ali L, Knight T M and Pullin A S 2010 Urban greening to cool towns and cities: a systematic review of the empirical evidence *Landscape Urban Plan.* **97** 147–55

[40] Wang Z H, Zhao X, Yang J and Song J 2016 Cooling and energy saving potentials of shade trees and urban lawns in a desert city *Appl. Energy* **161** 437–44